Environmental Science Advances

ROYAL SOCIETY OF CHEMISTRY

PAPER

View Article Online
View Journal | View Issue

Cite this: *Environ. Sci.: Adv.*, 2026, **5**, 809

Preparation of irregularly shaped, nano-sized, fluorescent microplastic particles for tracing cellular uptake

Ryo Nagasawa,[a] Sota Inoue,[a] Takashi Miyano[b] and Masakazu Umezawa *[ab]

Microplastics (MPs) are widely distributed; however, their behaviour in the environment and within biological tissues remains unclear. Concerns regarding their health risks have outpaced the elucidation of the true impacts of MPs. Previous studies have indicated that the toxicity of MPs depends on their size. However, toxicity assessments have mainly focused on uniformly sized, spherical polystyrene beads. Therefore, in this study, we developed a simple method for preparing irregularly shaped, nano-sized, fluorescent MP model particles. Fluorescence was incorporated by loading Nile red dye into plastics with various chemical compositions. Aqueous solution of bovine serum albumin (BSA) and chloroform solution of Nile red were added to solutions of polypropylene (PP), polyethylene (PE), and polyethylene terephthalate (PET) fragmented to nanoscale *via* solvent-assisted degradation in an organic solvent. Subsequently, model particles of MPs with diameters of 80–250 nm were obtained by volatilising the organic solvent. The BSA functioned as a weak surfactant to prepare irregularly shaped, nano-sized MP particles. Organic solvents with solubility parameters close to those of the plastic materials proved useful for fragmenting durable solvent-treated plastic polymers. Experiments using Nile red incorporated into PP, PE, and PET yielded model particles of PP, PE, and PET that emitted fluorescence at 580–620 nm under 550 nm excitation. The fluorescence of Nile red-loaded nano-MP particles enabled microscopic observation of their cellular uptake. The method presented herein for fabricating fluorescent nano-MP particles using albumin will contribute to further comparative studies of environmental and *in vivo* MP behaviours.

Received 16th January 2026
Accepted 9th February 2026

DOI: 10.1039/d6va00031b

rsc.li/esadvances

Environmental significance

Visualizing the environmental and *in vivo* behaviour of microplastics (MPs) is needed to address public concerns about MP issues. However, significant data gaps remain regarding the behaviour of irregularly shaped nanoscale MPs (nano-MPs). This study presents a method for preparing irregularly shaped, fluorescent nano-MP model particles to enable microscopic observation of their cellular uptake. This method for fabricating fluorescent nano-MPs using albumin will contribute to further comparative studies on the behaviour of MPs.

Introduction

Plastic pollution in marine, soil, and atmospheric environments has attracted global attention.[1] In addition to the accumulation of large, visible debris, the presence of micro- and nano-scale plastic particles used in industrial processes or commercial products, or originating from the degradation of daily use objects, has been reported.[2] These small particles, with sizes ranging from millimetres (<5 mm) to nanometres, are known as microplastics (MPs). Recently, MPs have been recognised as emerging particulate pollutants in all environmental compartments.[3] The presence of large quantities of nano-sized MPs (nano-MPs) in the air has not been adequately quantified, but knowledge has been accumulated since 2015. Household air dust analyses have shown that the contamination of indoor environments by MPs may cause hygiene problems.[4] Owing to their chemical inertness, long-term environmental persistence of MPs has been observed. In addition to the potential biological effects on the survival and health of various species,[5,6] humans are chronically exposed to MPs through ingestion and inhalation, and the outcome of such exposure remains unclear.[7–10]

One of the biggest challenges in MP research is observing their environmental and *in vivo* behaviour and fate. Notably, MPs have been detected in fruits and vegetables,[11] seafood,[12]

[a]*Department of Materials Science and Technology, Graduate School of Advanced Engineering, Tokyo University of Science, 6-3-1 Niijuku, Katsushika, Tokyo 125-8585, Japan. E-mail: masa-ume@rs.tus.ac.jp*

[b]*Department of Medical and Robotic Engineering Design, Faculty of Advanced Engineering, Tokyo University of Science, 6-3-1 Niijuku, Katsushika, Tokyo 125-8585, Japan*

drinking water,[13] and table salt.[14] The inhalation of airborne MP particles[15] has also been reported, and MPs have been detected in human blood[16] and faeces.[6] The environmental transport process and *in vivo* behaviour of MPs must be traced to accurately determine their bioaccumulation.[17] Previous studies have shown that in a sample of fibrous fallout passively collected from approximately 20 households in the United Kingdom, polyethylene terephthalate (PET) accounted for the highest proportion at 63%.[18] Meanwhile, PET, polytetrafluoroethylene, polymethyl methacrylate, polypropylene (PP), and polyvinyl chloride (PVC) accounted for 72% of all Western Pacific MPs, with PET accounting for over 30% at each sample collection site.[19] Furthermore, polyester, PP, and polyethylene (PE) were detected in air samples from the Baltic Sea coast at rates of 41%, 18%, and 14%, respectively.[20] In a report quantifying MPs over a large area covering most of Europe, PET accounted for the highest percentage (15%) of MPs in sediments and in the ocean, and PP accounted for more than 13%, which showed the highest percentages.[21] In the natural environment, large plastic wastes undergo progressive degradation through the combined action of physical, chemical and biological processes such as photo-oxidation and ensuing thermally activated reactions, mechanical abrasion, and microbial activity. These processes cause surface oxidation and embrittlement of polymers, leading to fragmentation into nano- and MPs over a long period of time.[22] Ingestion of MPs by soil fauna causes poor nutrient supply, oxidative stress, intestinal damage,[23] and increased mortality.[24] Furthermore, ingested MPs accumulate within the food chain, harming organisms at higher trophic levels.[25] Owing to the large number of MPs in the atmosphere, humans are also exposed through inhalation, potentially causing health risks such as oxidative stress and inflammatory damage, while the atmospheric concentration can affect MP ingestion, metabolism, and residence.[26]

The size, composition, morphology, aging time, and surface properties of plastic particles are closely associated with their adverse effects on organisms. Particle size is the most important factor in determining the biodistribution and toxicity.[27] In general, the smaller the particle size and the larger the specific surface area of nanoparticles, the more their penetration into an organism and, therefore, the more toxic they are. Previous studies have shown that MPs, including nano-MPs, can accumulate in living organisms and be distributed in the liver, spleen, lungs, blood, and testes, and the absorption and biodistribution of plastic particles by organisms increase with decreasing particle size.[28,29] Polystyrene (PS; 100 nm) may be absorbed into the blood and may be more likely to be toxic than larger MPs.[30] It has been found that nano-MPs may have toxic effects on marine and freshwater organisms, including bacteria such as planaria, zebrafish, and fathead minnows.[31–33] Particles that are <150 μm in diameter are more likely to cross the gut mucosal barrier, and only particles with a diameter <1.5 μm are transported to deeper tissues.[34,35] Plastic particles that are <200 nm in diameter are more likely to accumulate in organs such as the liver, lungs, spleen, and kidneys. NP accumulation depended on size. Smaller NP can reach internal organs (brain, eyes, liver, pancreas, heart) but larger (>200 nm) accumulate mainly in gut, gills and skin.[36] However, it is currently unclear how irregularly shaped nano-sized MPs enter the human body and how they can damage various organs of the human body.[37] Previous MP studies have mainly focused on spherical PS and PE particles because of easy access to commercial products.[38,39] However, commonly used commercial spherical MP samples do not represent the particle morphology in the environment.

The development of small, irregularly shaped MPs has been challenging. Additionally, many staining methods lack interpolymer applicability. Previous Nile red-based methods have been used for the high-throughput detection of environmental MPs, but have typically targeted micrometre-scale, fragment-like particles or relied on PS spheres. Bovine serum albumin (BSA)-assisted incorporation protocols for producing irregularly shaped, submicrometre-scale, Nile red-labelled particles from PE, PP, and PET have also been investigated.[40,41]

The effects of spherical plastic particles on living organisms are likely to differ from those of environmental MPs because of their shape characteristics. Notably, MPs found in aquatic environments are irregularly shaped because of the effects of weathering and crushing. The effects of spherical and irregularly shaped MPs on green medaka (*Cyprinodon variegatus*) were compared, and irregularly shaped MPs were found to reduce swimming behaviour compared with spherical MPs.[42] The MPs identified in the digestive tracts of marine fish are highly variable in shape and roughness.[43] PP-MP fibres have been reported to be more harmful to *Hyalella azteca* (freshwater amphipod) than spherical particles because of their longer residence times in the gut.[44] Plastics prepared using strong surfactants are spherical in shape, but this does not mimic the shape of environmental MPs. Therefore, in this study, preparation was carried out using albumin protein, which works as a weak surfactant, to obtain irregularly shaped nano-MP models. Fluorescence was introduced by loading Nile red dye into the PP, PE, and PET MPs during preparation. The aim of this study was to develop a protocol for the preparation of fluorescent nano-MPs with irregular shapes to trace their intracellular behaviour.

Experimental

Materials

Plastic granules of PET, PE, PP, BSA, and penicillin–streptomycin mixture (P/S; 10 000 units penicillin and 10 mg streptomycin per mL) were purchased from Sigma-Aldrich (MO, USA). Acetonitrile (ACN), tetrahydrofuran (THF), chloroform, and Dulbecco's modified Eagle medium (D-MEM) were purchased from Fujifilm Wako Pure Chemical Industries (Osaka, Japan). Nile red was purchased from Tokyo Chemical Industry (Tokyo, Japan). Gibco fetal bovine serum (FBS) was purchased from Thermo Fisher Scientific Inc. (MA, USA). All reagents were used without further purification.

Preparation of Nile red-loaded MPs

The PE and PP granules were fragmented in THF, whereas the PET granules were fragmented in ACN as similar to the previous

studies.[45] Fragmentation resulted in smaller particles of several tens of nanometres. The fragmented nanometre-scale polymers from the starting granules appear in the supernatant, which was collected gently. A part of the collected supernatant was dried in air, and the residue was weighed using an analytical balance (AUW120D; Shimadzu Co., Kyoto, Japan) to determine the concentration of the fragmented polymer. Subsequently, the solvent (THF or ACN) was added to the remaining supernatant to prepare a 2 mg mL^{-1} fragmented polymer dispersion. The fragmented PE, PP, and PET (2 mg mL^{-1}, 2 mL) were mixed with Nile red dissolved in chloroform (0.01 μg mL^{-1}, 1 mL). Therefore, the mass ratio of MPs to Nile red ranged from 400 000 to 1. Then, an aqueous solution of BSA (6.25 mg mL^{-1}) was added dropwise into the mixture of fragmented plastics and Nile red and stirred for 48 h in an open system at 25 °C to remove the organic solvents *via* evaporation (Fig. 1). Nile red-loaded MPs were produced in water through the function of BSA as a weak surfactant.

Characterisation of Nile red-loaded MPs

The hydrodynamic size of the MPs was analysed using dynamic light scattering (DLS; ELSZ-2000 ZS, Otsuka Electronic Co., Osaka, Japan). The size and morphology of the particles were analysed through transmission electron microscopy (TEM; H-7650, Hitachi High-Tech, Tokyo, Japan). A part of the Nile red-loaded MP dispersion was dried, and the residue was weighed using the analytical balance to determine the concentration of fluorescent MPs per volume in the dispersion. The fluorescence spectra of the MPs were analysed using a spectrometer (RF-5300, Shimadzu Co., Kyoto, Japan).

Cell culture and fluorescent microscopy

Mouse fibroblasts (3T3-L1) were cultured in D-MEM containing 10% FBS and 1% P/S in 35 mm glass-bottom dishes under 5% CO_2 in an incubator. When the cells reached sub-confluency, they were treated with a medium containing Nile red-loaded MPs (2.0 μg mL^{-1}) for 30 min. Then, the cells were washed with PBS to observe fluorescence images (wavelength 630 ± 37.5 nm) using Thunder Imaging Systems (DMi8, Leica Microsystems Co., Germany) under optical excitation at a wavelength of 560 ± 20 nm.

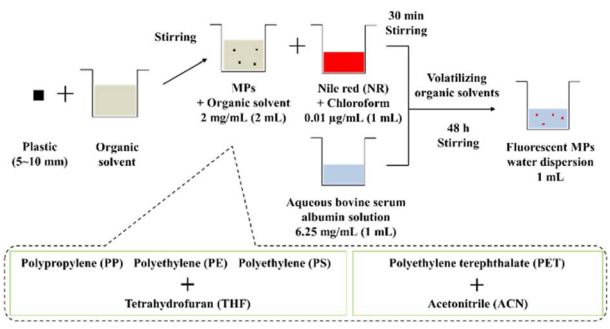

Fig. 1 Schematic illustration of the preparation of the Nile red-loaded nano-microplastic (MP) particle model.

Results

Particle size of generated nano-MPs

Using polymer fragmentation in THF or ACN followed by the controlled addition of an aqueous BSA solution and solvent evaporation, we generated irregularly shaped fluorescent nano-MPs from PE, PP, and PET. We confirmed their nano-scale size distribution through DLS/TEM analyses (Fig. 2). The DLS measurements showed that the hydrodynamic diameters of fluorescent PP and PE were in the range of 80–1000 nm, while that of PET was in the range of 100–500 nm dispersed in water (Fig. 2a). The TEM images showed the presence of a mixture of particles <100 nm and those several hundred nm in diameter for each of the three compositions. As observed through TEM, the generated nano-MPs were irregularly shaped rather than spherical (Fig. 2b–d).

Fluorescence properties of Nile red-loaded nano-MPs

While Nile red shows fluorescence at 590 nm upon excitation with light (550 nm), the dye-loaded MPs showed fluorescence peaks at slightly different wavelengths. The fluorescence of the PET MPs peaked at 580 nm, whereas that of the PP and PE MPs peaked at 610 nm (Fig. 2e). This difference was likely due to the solvatochromism of Nile red in plastics and solvents,[46] and a similar change in the fluorescence wavelength of Nile red has been observed when it is dissolved in lipids with different polarities.[47]

In this study, MPs of multiple chemical compositions (PP, PE, and PET) were experimentally prepared with various shapes and sizes in the range of tens to hundreds of nanometres by

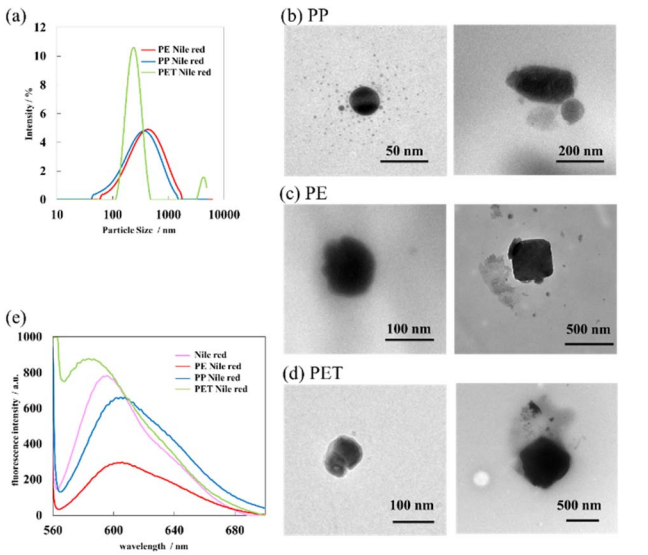

Fig. 2 Characterisation of fluorescent nano-MP particles prepared with albumin. (a) Size distribution determined through dynamic light scattering (DLS). Transmission electron microscopy (TEM) images of (b) polypropylene (PP), (c) polyethylene (PE), and (d) polyethylene terephthalate (PET) nano-MP particles. (e) Fluorescence spectra of the prepared nano-MP particles analysed under optical excitation (550 nm).

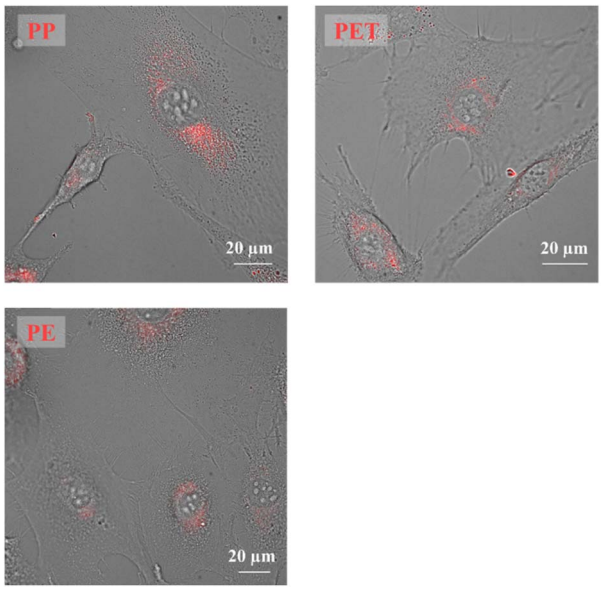

Fig. 3 Fluorescence images of mouse fibroblasts (3T3-L1) treated with Nile red-loaded nano-MPs of PP, PE, and PET (2 μg mL^{-1}) under optical excitation at 560 ± 20 nm.

fragmenting commercial plastic beads and adding a weak surfactant (BSA). After introducing Nile red, the nano-MPs showed fluorescence at 580 nm (PET) and 610 nm (PE and PP), which is consistent with the dye's solvatochromism. These results indicate that this protocol is suitable for preparing visually trackable and environmentally relevant nano-MP models for uptake and biodistribution studies.

Fluorescence microscopy of cellular uptake of Nile red-loaded nano-MPs

We observed the cellular uptake of fluorescent MPs by 3T3-L1 cells using fluorescence microscopy. The cells were incubated with the MPs for 30 min. The fluorescence of Nile red-loaded nano-MPs was localised in the cytoplasm, and MPs were not found in the nucleus (Fig. 3). Fluorescent nano-MPs taken up by the cells appeared to be concentrated in clusters around the nucleus. These images suggest that MPs are transported into the cells *via* endocytic pathways.

Discussion

In this study, plastic granules were fragmented in organic solvents to prepare irregularly shaped nano-MPs loaded with fluorescent dye. The selected polymers are thermoplastic materials and their strength derives from the semi-crystalline regions, which act as physical restraints rather than covalent cross-linking. To obtain the nanometre-scale polymer dispersions from the beginning materials, solvents close to the solubility parameters of the plastic materials were employed.

As shown in Table 1, the solubility parameter of THF matched those of PE and PP, whereas that of PET was closer to that of ACN; therefore, these combinations were adopted in the study protocol. This strategy predicts that the plastic granules will undergo a solvent-assisted degradation process involving swelling of the amorphous polymer regions rather than dissolution of the crystalline regions. This would result in partial extraction of weakly constrained polymer fraction and colloidal re-precipitation following solvent exchange into a water-soluble BSA solution, producing ultrafine particles on the tens of nanometre scale.

Table 1 Solubility parameters of plastics and solvents used in this study

Plastics/solvents	Solubility parameter[55]
Polyethylene (PE)	8.6
Polypropylene (PP)	9.1
Polyethylene terephthalate (PET)	11.0
Tetrahydrofuran (THF)	9.1
Acetonitrile (ACN)	12.2

Compared with commercially produced spherical MPs, nano-MPs formed through weathering and degradation in the environment exhibit improved dispersibility in aquatic environments such as the ocean. Therefore, model MPs that are experimentally fabricated to mimic environmental nano-MPs should ideally have hydrophilic surfaces. When the solvent evaporates after the addition of water without surfactants, the fragmented plastic forms large lumps. In contrast, in the presence of surfactants in water, hydrophobic molecules are incorporated into the surfactant to form nano-sized particles. In this case, albumin protein was used as a weak surfactant to achieve irregularly shaped particle formation. It coated the particle surface and served as a model for the microbial layer dispersing nano-MPs in aqueous environments.

The detection of MPs through fluorescent labelling of plastic fragments is becoming increasingly popular as a convenient tracking method.[48–50] Some fluorescent dyes interact with plastic fragments, enabling their visualisation. Nile red, a lipophilic fluorescent dye commonly used for *in situ* lipid staining, has been used to stain plastic fragments in environmental samples through hydrophobic interactions.[40,41,51] Furthermore, in exposure experiments,[52] Nile red derivatives dissolved in acetone have been used to improve the staining accuracy of PE, PP, and PVC plastic fragments.[50] Meanwhile, a unique trackable MP model was proposed by incorporating magnetic iron oxide into the MP core, although the density may change owing to the internalisation of the metal oxide.[53]

The method used in the current study was shown to be suitable for preparing fluorescent nano-MP model particles with three different chemical compositions (PP, PE, and PET). Using an organic solvent with a solubility parameter close to that of plastic, the dissolved dye can be introduced into the MP. While many previous studies have used acetone as the solvent for Nile red dye, and dissolving it in THF (or ACN) enables efficient dye loading into plastic particles. The quality of Nile red loading in this study is sufficient for qualitative to semi-quantitative visualization of MPs' cellular uptake. However, in this study, the loading process was just evaluated primarily

based on reproducible fluorescent signals and suitability for visualizing particle uptake into cells. Further investigations are needed to control the number concentration of administered particles, a necessary step to ensure realistic applied dose and thus realistic corresponding responses, and to evaluate uniform dye loading to MPs for absolute quantitative analysis of their cellular uptake. Although potential desorption of the dye loaded in prepared fluorescent nano-MPs in aqueous suspension was not assessed; however, the samples were available for fluorescence microscopy at several months after preparation. Therefore, quenching due to the dye desorption seemed to be minimized.

The irregularly shaped, Nile red-loaded, fluorescent nano-MP models prepared in this study emitted fluorescence at wavelengths of 580–620 nm under 550 nm light excitation. A limitation of this protocol is that fluorescence cannot be introduced into plastics with a low chemical affinity for Nile red. However, this limitation can be overcome by utilising other hydrophobic fluorescent dyes such as iDye,[38] 4-dimethylamino-4′-nitrostilbene,[49] graphite-like carbon nitride,[54] or fluorescent polymeric carbon nitride.[54] In this study, we demonstrated that Nile red is effective for the fluorescent labelling of PE and PP (when used with THF), which are frequently used in MP studies, as well as PET (when used with ACN), a material with a chemical composition common in the environment.

This preparation approach shown in this study has limitations in the precise control of particle shape and size. Indeed, the variability of the particle size range and the difficulty in reproducing shape control during the preparation process may limit its use as a reference material in toxicity testing. Rather, it allows to produce nano- and micro-plastics with heterogeneous and irregular shapes that approximate the morphological diversity found in environmental particles. However, as they do not reproduce the physicochemical history or internal structure of environmental nanoplastics, they are designed as feature-based model particles focusing on properties commonly observed in environmental micro- and nanoplastics. Also, environmental nanoplastics are widely considered to be highly crystalline residues formed through long-term environmental degradation processes in which amorphous regions are preferentially degraded, while the solvent-assisted degradation and reprecipitation method used in this study may produce particles with lower crystallinity and a different structural history. The advantage of our method is to produce fluorescent nano-MPs with a broad particle size distribution and morphological heterogeneity intentionally reflect the polydispersity of environmental particles, while internal crystallinity and degradation history are outside the scope of this model.

Conclusions

This study presents a method for preparing fluorescent nano-sized MP model particles to enable the analysis of the environmental and *in vivo* processes and fates of nano-sized plastic particles. Most previous studies on nano-MP toxicity have used spherical nano-MPs, which differ in shape from the MPs found in the environment. In contrast, this study demonstrates a protocol using albumin protein, a weak surfactant, for preparing irregularly shaped, nano-sized MP particle models. Organic solvents with solubility parameters close to those of the plastic material proved useful for fragmenting durable solvent-treated plastic polymers and converting them into nano-sized plastic particles. The addition of Nile red dye to the organic solvent during particle preparation provided nano-MP model particles that emitted fluorescence at 580–620 nm under optical excitation at 550 nm. Spectroscopic and microscopic characterisations confirmed robust dye incorporation and size control, supporting its application in cellular uptake assays. The fluorescence of Nile red-loaded nano-MPs enabled microscopic observation of their cellular uptake. This method for fabricating fluorescent nano-MPs using albumin will contribute to further comparative studies on the environmental and *in vivo* behaviour of MPs.

Author contributions

MU is the leader of this research and conceived the overall research idea. RN conducted all the experiments with SI, data collection, and data analysis. TM substantially contributed to fluorescence microscopy of cells. The manuscript was drafted by RN and edited by MU. All the authors have read the final version of the manuscript and approved the submission.

Conflicts of interest

The authors have no conflicts of interest to declare.

Data availability

Data to reproduce the figures of this article are available at https://tus.box.com/s/1xbyqefq74zvlyunlaxx699ww5we3pg3.

Acknowledgements

This work was in part supported by JSPS KAKENHI (Grant Numbers 22H03335, 22K06565 and 25K02871).

References

1 A. L. Andrady, Microplastics in the marine environment, *Mar. Pollut. Bull.*, 2011, **62**(8), 1596–1605.
2 S. Anbumani and P. Kakkar, Ecotoxicological effects of microplastics on biota: a review, *Environ. Sci. Pollut. Res.*, 2018, **25**(15), 14373–14396.
3 S. Sridharan, M. Kumar, L. Singh, N. S. Bolan and M. Saha, Microplastics as an emerging source of particulate air pollution: A critical review, *J. Hazard. Mater.*, 2021, **418**, 126245.
4 T. Salthammer, Microplastics and their additives in the indoor environment, *Angew. Chem.*, 2022, **134**(32), e202205713.
5 C. M. Boerger, G. L. Lattin, S. L. Moore and C. J. Moore, Plastic ingestion by planktivorous fishes in the North

Pacific Central Gyre, *Mar. Pollut. Bull.*, 2010, **60**(12), 2275–2278.
6 E. L. Ng, E. H. Lwang, S. M. Eldridge, P. Johnston, H. W. Hu, V. Geissen and D. Chen, An overview of microplastic and nanoplastic pollution in agroecosystems, *Sci. Total Environ.*, 2018, **627**, 1377–1388.
7 M. Smith, D. C. Love, C. M. Rochman and R. A. Neff, Microplastics in seafood and the implications for human health, *Curr. Environ. Health Rep*, 2018, **5**(3), 375–386.
8 W. Wang, H. Gao, S. Jin, R. Li and G. Na, The ecotoxicological effects of microplastics on aquatic food web, from primary producer to human: A review, *Ecotoxicol. Environ. Saf.*, 2019, **173**, 110–117.
9 G. Bhardwaj, M. Abdulkadhim, K. Joshi, L. Wankhede, R. K. Das and S. K. Brar, Exposure Pathways, Systemic Distribution, and Health Implications of Micro- and Nanoplastics in Humans, *Appl. Sci.*, 2025, **15**(16), 8813.
10 M. H. Lamoree, J. van Boxel, F. Nardella, K. J. Houthuijs, S. H. Brandsma, F. Béen and M. B. M. van Duursen, Health impacts of microplastic and nanoplastic exposure, *Nat. Med.*, 2025, **31**, 2873–2887.
11 G. O. Conti, M. Ferrante, M. Banni, C. Favara, I. Nicolosi, A. Cristaldi, M. Fiore and P. Zuccarello, Micro-and nanoplastics in edible fruit and vegetables. The first diet risks assessment for the general population, *Environ. Res.*, 2020, **187**, 109677.
12 EFSA Panel on Contaminants in the Food Chain (CONTAM), Presence of microplastics and nanoplastics in food, with particular focus on seafood, *EFSA J.*, 2016, **14**(6), e04501.
13 S. A. Mason, V. G. Welch and J. Neratko, Synthetic polymer contamination in bottled water, *Front. Chem.*, 2018, **6**, 407.
14 D. Yang, H. Shi, L. Li, J. Li, K. Jabeen and P. Kolandhasamy, Microplastic pollution in table salts from China, *Environ. Sci. Technol.*, 2015, **49**(22), 13622–13627.
15 J. Domenech and R. Marcos, Pathways of human exposure to microplastics, and estimation of the total burden, *Curr. Opin. Food Sci.*, 2021, **39**, 144–151.
16 H. A. Leslie, M. J. Van Velzen, S. H. Brandsma, A. D. Vethaak, J. J. Garcia-Vallejo and M. H. Lamoree, Discovery and quantification of plastic particle pollution in human blood, *Environ. Int.*, 2022, **163**, 107199.
17 C. Song, X. Meng, Y. Liu, A. Shen, C. Shao, K. Wang, H. Cheng, X. Fang, P. Wang and W. Bu, Susceptibility-weighted imaging for metabolic pathway mapping of low-dosage nanoparticles in organisms, *Biomaterials*, 2020, **230**, 119631.
18 L. C. Jenner, L. R. Sadofsky, E. Danopoulos and J. M. Rotchell, Household indoor microplastics within the Humber region (United Kingdom): Quantification and chemical characterisation of particles present, *Atmos. Environ.*, 2021, **259**, 118512.
19 D. Li, K. Liu, C. Li, G. Peng, A. L. Andrady, T. Wu, Z. Zhang, X. Wang, Z. Song, C. Zong and F. Zhang, Profiling the vertical transport of microplastics in the West Pacific Ocean and the East Indian Ocean with a novel in situ filtration technique, *Environ. Sci. Technol.*, 2020, **54**(20), 12979–12988.
20 K. Szewc, B. Graca and A. Dołęga, Atmospheric deposition of microplastics in the coastal zone: Characteristics and relationship with meteorological factors, *Sci. Total Environ.*, 2021, **761**, 143272.
21 E. E. Burns and A. B. Boxall, Microplastics in the aquatic environment: Evidence for or against adverse impacts and major knowledge gaps, *Environ. Toxicol. Chem.*, 2018, **37**(11), 2776–2796.
22 H. Luo, Z. Li, Y. Zeng, D. He, J. Sun, A. Zhang and X. Pan, Degradation of microplastics in the natural environment: A comprehensive review on process, mechanism, influencing factor and leaching behavior, *J. Environ. Manage.*, 2025, **391**, 126429.
23 Y. Zhang, X. Zhang, X. Li and D. He, Interaction of microplastics and soil animals in agricultural ecosystems, *Curr. Opin. Environ. Sci. Health*, 2022, **26**, 100327.
24 J. Li, Y. Song and Y. Cai, Focus topics on microplastics in soil: Analytical methods, occurrence, transport, and ecological risks, *Environ. Pollut.*, 2020, **257**, 113570.
25 S. Bejgarn, M. MacLeod, C. Bogdal and M. Breitholtz, Toxicity of leachate from weathering plastics: An exploratory screening study with Nitocra spinipes, *Chemosphere*, 2015, **132**, 114–119.
26 C. D. Dong, C. W. Chen, Y. C. Chen, H. H. Chen, J. S. Lee and C. H. Lin, Polystyrene microplastic particles: In vitro pulmonary toxicity assessment, *J. Hazard. Mater.*, 2020, **385**, 121575.
27 V. Stock, L. Böhmert, E. Lisicki, R. Block, J. Cara-Carmona, L. K. Pack, R. Selb, D. Lichtenstein, L. Voss, C. J. Henderson and E. Zabinsky, Uptake and effects of orally ingested polystyrene microplastic particles in vitro and in vivo, *Arch. Toxicol.*, 2019, **93**(7), 1817–1833.
28 B. Liang, Y. Zhong, Y. Huang, X. Lin, J. Liu, L. Lin, M. Hu, J. Jiang, M. Dai, B. Wang and B. Zhang, Underestimated health risks: polystyrene micro-and nanoplastics jointly induce intestinal barrier dysfunction by ROS-mediated epithelial cell apoptosis, *Part. Fibre Toxicol.*, 2021, **18**(1), 20.
29 Y. Deng, Y. Zhang, B. Lemos and H. Ren, Tissue accumulation of microplastics in mice and biomarker responses suggest widespread health risks of exposure, *Sci. Rep.*, 2017, **7**(1), 46687.
30 B. Du, T. Li, H. He, X. Xu, C. Zhang, X. Lu, Y. Wang, J. Cao, Y. Lu, Y. Liu and S. Hu, Analysis of biodistribution and in vivo toxicity of varying sized polystyrene micro and nanoplastics in mice, *Int. J. Nanomed.*, 2024, **19**, 7617–7630.
31 T. Gao, B. Sun, Z. Xu, Q. Chen, M. Yang, Q. Wan, L. Song, G. Chen, C. Jing, E. Y. Zeng and G. Yang, Exposure to polystyrene microplastics reduces regeneration and growth in planarians, *J. Hazard. Mater.*, 2022, **432**, 128673.
32 J. A. Pitt, J. S. Kozal, N. Jayasundara, A. Massarsky, R. Trevisan, N. Geitner, M. Wiesner, E. D. Levin and R. T. Di Giulio, Uptake, tissue distribution, and toxicity of polystyrene nanoparticles in developing zebrafish (Danio rerio), *Aquat. Toxicol.*, 2018, **194**, 185–194.
33 A. C. Greven, T. Merk, F. Karagöz, K. Mohr, M. Klapper, B. Jovanović and D. Palić, Polycarbonate and polystyrene nanoplastic particles act as stressors to the innate immune

system of fathead minnow (Pimephales promelas), *Environ. Toxicol. Chem.*, 2016, **35**(12), 3093–3100.
34 N. Hussain, V. Jaitley and A. T. Florence, Recent advances in the understanding of uptake of microparticulates across the gastrointestinal lymphatics, *Adv. Drug Delivery Rev.*, 2001, **50**(1–2), 107–142.
35 J. W. Yoo, N. Doshi and S. Mitragotri, Adaptive micro and nanoparticles: temporal control over carrier properties to facilitate drug delivery, *Adv. Drug Delivery Rev.*, 2011, **63**(14–15), 1247–1256.
36 M. T. Ruiz, A. D. l. Vieja, M. de. A. Gonzalez, M. E. Lopez, A. C. Calvo and A. I. C. Portilla, Toxicity of nanoplastics for zebrafish embryos, what we know and where to go next, *Sci. Total Environ.*, 2021, **797**(25), 149125.
37 X. Yao, X. S. Luo, J. Fan, T. Zhang, H. Li and Y. Wei, Ecological and human health risks of atmospheric microplastics (MPs): a review, *Environ. Sci.: Atmos.*, 2022, **2**(5), 921–942.
38 E. G. Karakolis, B. Nguyen, J. B. You, C. M. Rochman and D. Sinton, Fluorescent dyes for visualizing microplastic particles and fibers in laboratory-based studies, *Environ. Sci. Technol. Lett.*, 2019, **6**(6), 334–340.
39 G. Chen, Z. Fu, H. Yang and J. Wang, An overview of analytical methods for detecting microplastics in the atmosphere, *TrAC, Trends Anal. Chem.*, 2020, **130**, 115981.
40 W. J. Shim, Y. K. Song, S. H. Hong and M. Jang, Identification and quantification of microplastics using Nile Red staining, *Mar. Pollut. Bull.*, 2016, **113**(1–2), 469–476.
41 T. Maes, R. Jessop, N. Wellner, K. Haupt and A. G. Mayes, A rapid-screening approach to detect and quantify microplastics based on fluorescent tagging with Nile Red, *Sci. Rep.*, 2017, **7**(1), 44501.
42 J. S. Choi, Y. J. Jung, N. H. Hong, S. H. Hong and J. W. Park, Toxicological effects of irregularly shaped and spherical microplastics in a marine teleost, the sheepshead minnow (Cyprinodon variegatus), *Mar. Pollut. Bull.*, 2018, **129**(1), 231–240.
43 D. Mazurais, B. Ernande, P. Quazuguel, A. Severe, C. Huelvan, L. Madec, O. Mouchel, P. Soudant, J. Robbens, A. Huvet and J. Zambonino-Infante, Evaluation of the impact of polyethylene microbeads ingestion in European sea bass (Dicentrarchus labrax) larvae, *Mar. Environ. Res.*, 2015, **112**, 78–85.
44 S. Y. Au, T. F. Bruce, W. C. Bridges and S. J. Klaine, Responses of Hyalella azteca to acute and chronic microplastic exposures, *Environ. Toxicol. Chem.*, 2015, **34**(11), 2564–2572.
45 S. Inoue, T. Isobe, K. Soga and M. Umezawa, Near-infrared (NIR-II) fluorescent poly(ethylene terephthalate) nano-microplastics for in vivo tracking, *J. Nanopart. Res.*, 2025, **28**, 5.
46 P. Greenspan and S. D. Fowler, Spectrofluorometric studies of the lipid probe, nile red, *J. Lipid Res.*, 1985, **26**(7), 781–789.
47 W. Teo, A. V. Caprariello, M. L. Morgan, A. Luchicchi, G. J. Schenk, J. T. Joseph, J. J. Geurts and P. K. Stys, Nile Red fluorescence spectroscopy reports early physicochemical changes in myelin with high sensitivity, *Proc. Natl. Acad. Sci. U. S. A.*, 2021, **118**(8), e2016897118.
48 V. C. Shruti, F. Pérez-Guevara, P. D. Roy and G. Kutralam-Muniasamy, Analyzing microplastics with Nile Red: Emerging trends, challenges, and prospects, *J. Hazard. Mater.*, 2022, **423**, 127171.
49 G. Sancataldo, V. Ferrara, F. P. Bonomo, D. F. Chillura Martino, M. Licciardi, B. G. Pignataro and V. Vetri, Identification of microplastics using 4-dimethylamino-4′-nitrostilbene solvatochromic fluorescence, *Microsc. Res. Tech.*, 2021, **84**(12), 2820–2831.
50 M. T. Sturm, E. Myers, D. Schober, A. Korzin and K. Schuhen, Development of an inexpensive and comparable microplastic detection method using fluorescent staining with novel nile red derivatives, *Analytica*, 2023, **4**(1), 27–44.
51 G. Erni-Cassola, M. I. Gibson, R. C. Thompson and J. A. Christie-Oleza, Lost, but found with Nile red: a novel method for detecting and quantifying small microplastics (1 mm to 20 μm) in environmental samples, *Environ. Sci. Technol.*, 2017, **51**(23), 13641–13648.
52 M. Cole, A novel method for preparing microplastic fibers, *Sci. Rep.*, 2016, **6**(1), 34519.
53 L. Zhang, H. Liu, Q. Xin, L. Tang, J. Tang, Y. Liu and L. Hu, A quantitative study of nanoplastics within cells using magnetic resonance imaging, *Sci. Total Environ.*, 2023, **886**, 164033.
54 X. Zheng, Q. Feng, J. Chen, J. Yan, X. Li and L. Guo, Quantification analysis of microplastics released from disposable polystyrene tableware with fluorescent polymer staining, *Sci. Total Environ.*, 2023, **864**, 161155.
55 M. Singla, J. Díaz, F. Broto-Puig and S. Borrós, Sorption and release process of polybrominated diphenyl ethers (PBDEs) from different composition microplastics in aqueous medium: Solubility parameter approach, *Environ. Pollut.*, 2020, **262**, 114377.